

Numerical Simulation of AC Plasma Arc Thermodynamics

HAN-MING WU

Institute of Mechanics, Academia Sinica, Beijing 100080, China

G. F. CAREY

*Computational Fluid Dynamics Laboratory, Department of Aerospace Engineering and Engineering Mechanics,
The University of Texas at Austin, Texas 78712*

AND

M. E. OAKES

Department of Physics, The University of Texas at Austin, Texas 78712

Received August 23, 1991; revised February 22, 1993

A mathematical model and approximate analysis for the energy distribution of an ac plasma arc with a moving boundary is developed. A simplified electrical conductivity function is assumed so that the dynamic behavior of the arc may be determined, independent of the gas type. The model leads to a reduced set of non-linear partial differential equations which governs the quasi-steady ac arc. This system is solved numerically and it is found that convection plays an important role, not only in the temperature distribution, but also in arc disruptions. Moreover, disruptions are found to be influenced by convection only for a limited frequency range. The results of the present studies are applicable to the frequency range of $10\text{--}10^2$ Hz which includes most industry ac arc frequencies. © 1994 Academic Press, Inc.

1. INTRODUCTION

Plasma arcs have received increasing attention recently for a variety of applications in engineering and physics [1-9]. There are mainly three types of plasma arcs—dc arcs, ac arcs and rf arcs. It is known that ac arcs offer certain advantages over rf plasma generators and dc devices; e.g., generation of ac arc plasma offer the possibility of easy scaling to higher power levels. Moreover, ac arc plasmas are also relevant to circuit breaker theory [3-5, 10].

Some of the recent work on ac arcs has been directed toward the study of arc heaters which involve high enthalpy gas flows. However, there has been relatively less work to date in this area compared with that available for dc arcs, since the ac arc physics is more complex, e.g., it is well known that there is a complex interaction between the arc temperature field and the surrounding flow field. Furthermore, the non-linear dependence of transport properties

upon temperature make analysis of the problem especially difficult.

The present work was initiated in an attempt to analyse and understand some of the fundamental processes that occur in an arc type of gas heater, employing an ac power supply. The details of this device, as well as some analytical investigations of its behavior have been reported in the literature [1, 6, 7, 9].

Moreover, there have been several related numerical studies, e.g., Ragaller *et al.* [3] developed a numerical model for studying the decay of a hot-gas channel after current-zero using transformed equations. A two-dimensional calculation based on the assumption of constant pressure in the radial direction was also made by Mitchell *et al.* [4]. In this latter model the evolution of the arc is followed from a steady state through the current ramp and during the subsequent free decay. Some related recent results are given in [5] under the assumption that radial gradients are negligible. In the present investigation we utilize the standard model [1], including nonlinear convective effects and with relaxed radial gradient assumptions. Hence this provides a more complete model of the physics that permits us to investigate convective effects more realistically during the entire interval of interest rather than only during the current ramp. The new model retains many of the features of previous models of this type and leads to an efficient decoupled solution algorithm suitable for PC and workstation computations.

Since the ac arc current is driven by the alternating voltage, it follows that temperature, density, and the extent of the plasma vary periodically. The fluctuation of the arc boundary does affect the arc properties and this case has

been previously examined [1, 7, 9]. However, the nature and importance of convective effects have received relatively little attention in previous work, although it has been suggested that convection might be significant [1]. Also, Wu and Chen [7] studied the convection problem with a direct variational method based on the assumption that the boundary position varies as $\rho = \rho_0 + \delta\rho \cos \omega t$, where ρ_0 is the average arc radius and $\delta\rho$ is an amplitude predetermined by some experimental results.

In the present paper, a cylindrically symmetric, dynamic, and wall-stabilized ac arc is considered. A mathematical model and approximate analysis is developed. The focus of the accompanying numerical studies is the non-linear convective effect. It is also shown that some ac arcs may be disrupted due to the effects of convection on the arc boundary oscillation.

2. MODEL OF THE PLASMA AC ARC

Let us consider the case when an ac arc discharges in a tube of radius R whose walls are maintained at a constant temperature without carrying current. A schematic diagram of the type of ac arc geometry considered in the present study is shown in Fig. 1. Regions I and II are the conducting and non-conducting zones, i.e., the arc column and transition regions, respectively. The domain is axisymmetric and the location of the boundary r_0 oscillates at the ac frequency. Since we are interested in the problem where heat conductivity κ depends on temperature T , it is convenient to introduce the heat flux potential

$$S = \int_{T_{ref}}^T \kappa(T) dT. \quad (1)$$

The electric conductivity σ of the gas and the heat flux

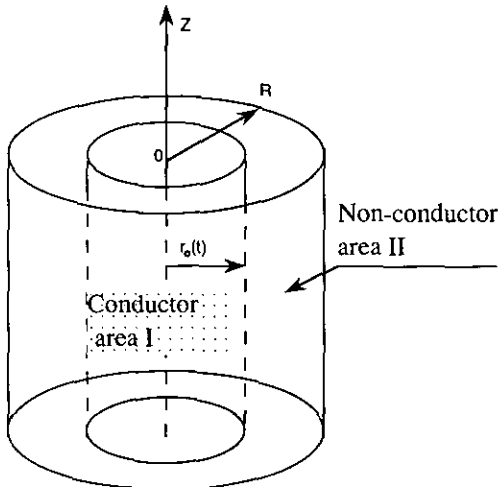


FIG. 1. Sketch of plasma arc cylinder.

potential S reach their maximum values at the arc center ($r=0$) and decrease with increasing r to $\sigma(r_0)=0$ and $S(r_0)=S_1$ (the value at which the gas begins to be ionized). It is known that the value S_1 depends mainly on the physical properties of the gas. For the purpose of the present analysis concerning dominant convective effects, we are able to make the following simplifying assumptions:

1. The arc is long enough that the end effects can be ignored;
2. The plasma geometry remains axially symmetric;
3. Heat transfer by radiation is negligible;
4. Any magnetic field induced by the arc current is insignificant;
5. The heat diffusivity $\lambda = \kappa/mc_p$ is a constant, where m and c_p are mass density and specific heat, respectively.
6. The electric conductivity σ is a linear function of the heat flux potential S :

$$\begin{aligned} \sigma &= 0, & r_0 \leq r \leq R \\ \sigma &= a(S - S_1), & 0 \leq r \leq r_0(t), \end{aligned} \quad (2)$$

where a and S_1 are known for the gas. For example, at pressure $p = 1$ atm: $a = 1.5$ mhos/W and $S_1 = 5$ W/cm for Ar; similarly, $a = 1$ mhos/W and $S_1 = 100$ W/cm for N_2 [1, 9]. In addition it is assumed that the arc gas is isobaric and quasi-neutral.

A result of the above assumptions is that the energy conservation equation combined with a suitable form of Ohm's law and mass conservation equation suffice to describe the arc column properties.

3. THE FUNDAMENTAL EQUATIONS

The preceding assumptions imply that the problem is cylindrically symmetric. Furthermore, in the absence of charge separation and an induced electric field, there is only an axial component to the total current and this is also independent of radius. The energy equation and mass equation in terms of S and T reduce to [7]

$$-\frac{v}{\lambda} \frac{\partial S}{\partial r} + \frac{1}{r} \frac{\partial}{\partial r} r \frac{\partial S}{\partial r} + a(S - S_1) \tilde{E}^2 = \frac{1}{\lambda} \frac{\partial S}{\partial t}, \quad 0 \leq r \leq r_0 \quad (3)$$

$$\frac{1}{r} \frac{\partial}{\partial r} r \frac{\partial S}{\partial r} - \frac{v}{\lambda} \frac{\partial S}{\partial r} = \frac{1}{\lambda} \frac{\partial S}{\partial t}, \quad r_0 \leq r \leq R \quad (4)$$

$$\frac{\partial(vr)}{r \partial r} - \frac{v}{T} \frac{\partial T}{\partial r} - \frac{1}{T} \frac{\partial T}{\partial t} = 0, \quad 0 \leq r \leq R, \quad (5)$$

where $\lambda = \kappa/mc_p$ is a heat diffusivity constant; \tilde{E} , T , v , κ , m , and c_p are the electric field, temperature, velocity, thermo-

conductivity, mass density, and specific heat, respectively [1, 9]. Note that Eq. (5) is derived from the mass conservation and perfect gas state equation and is decoupled from Eqs. (3)–(4) if the convective velocity vanishes.

We first introduce a transformation that eliminates the explicit dependence on the moving boundary. For the inner region (i.e., region I), the transformation takes the form

$$x = r/r_0(t), \quad 0 \leq r \leq r_0(t), \quad (6)$$

and for the outer region (i.e., region II)

$$y = \frac{R-r}{R-r_0(t)}, \quad r_0(t) \leq r \leq R, \quad (7)$$

so that both x and y range between zero and one.

Next, to construct a set of equations which may apply to any gas and facilitate comparison with other studies [1, 9], we introduce several dimensionless variables. In particular, let

$$\begin{aligned} U &= \frac{S-S_1}{S_1-S_2}, & 0 \leq r \leq r_0, \\ V &= \frac{S_1-S}{S_1-S_2}, & r_0 \leq r \leq R, \end{aligned} \quad (8)$$

where $S(r_0) = S_1$ and $S(R) = S_2$.

Finally, we introduce

$$\begin{aligned} \rho(t) &= r_0(t)/R, & E &= a^{1/2} R \bar{E}, & I &= \frac{\bar{I}}{(S_1-S_2) Ra^{1/2}} \\ \theta &= \frac{R^2}{\lambda}, & \tau &= \frac{t}{\theta}, \end{aligned} \quad (9)$$

where θ is the usual relaxation time scale for the heat conduction problem and \bar{I} denotes a value for the electric current.

Our main attention in the present study is focussed on the role of convection. Accordingly, let us simplify the problem as follows: Define an average value $\bar{\kappa}$ of thermo-conductivity based on the integral mean value so that from Eq. (1), $\bar{\kappa}T = S$ (if $T_{ref} = 0$). Then, Eqs. (2)–(4) can be expressed as

$$\rho^2 U_\tau = \frac{1}{x} (x U_x)_x + \frac{1}{2} \frac{d\rho^2}{dt} x U_x + \rho^2 E^2 U - v_1 \rho U_x \quad (10)$$

$$\rho_1^2 V_\tau = V_{yy} - \frac{\rho_1}{1-\rho_1 y} V_y - \frac{\rho_1}{2\rho} \frac{d\rho^2}{dt} y V_y - v_{II} \rho_1 V_y \quad (11)$$

$$v_{1x} = \frac{1}{U + C_I} (v_1 U_x - x \dot{\rho} U_x + \rho U_\tau) \quad (12)$$

$$v_{IIy} = \frac{1}{V + C_{II}} (v_{II} V_y - y \dot{\rho} V_y - \rho_1 V_\tau), \quad (13)$$

where

$$(1-\rho) U_x(1, \tau) = \rho V_y(1, \tau) \quad (14)$$

$$E = \frac{I}{2\pi\rho^2 \int_0^1 x U dx}, \quad I = I_d \cos \omega\theta\tau,$$

$$C_I = \frac{S_1}{S_1 - S_2} = -C_{II}, \quad \rho_1 = 1 - \rho, \quad \dot{\rho} = \frac{d\rho}{dt}.$$

Here, subscripts “ x ”, “ y ” and “ τ ” denote corresponding derivatives, and “I” and “II” refer to regions I and II (recall Fig. 1).

The boundary and initial conditions are, respectively,

$$\begin{aligned} U_x(0, \tau) &= 0, & U(1, \tau) &= 0, \\ V(0, \tau) &= 1, & V(1, \tau) &= 0 \\ v_{1x}(0, \tau) &= 0, & v_{II}(0, \tau) &= 0 \end{aligned}$$

and

$$\begin{aligned} U(x, 0) &= \frac{I_d J_0(\beta x)}{2\pi\rho_d J_1(\beta)} \\ V(y, 0) &= \frac{\ln((1-\rho_1 y)/\rho_d)}{\ln(1/\rho_d)} \\ I &= I_d = \frac{2\pi\rho_d}{\beta \ln(1/\rho_d)} \\ E &= E_d = \frac{\beta}{\rho_d}, \quad \rho = \rho_d, \end{aligned} \quad (15)$$

where J_0 and J_1 denote zero-order and first-order Bessel functions, and subscript “ d ” refers to the dc value.

4. NUMERICAL METHOD

We begin by noting that the linear stability condition for an explicit difference algorithm suggests that the timestep satisfy

$$\Delta\tau \leq \frac{1}{2} (1-\rho)^2 (\Delta y)^2,$$

where Δy is the grid size. In the present problem, as $r_0 \rightarrow R$, then $(1-\rho)$ will become very small. For example, in some applications $(1-\rho)$ may be less than 10^{-1} , and this implies that the time step must be less than $\frac{1}{2}(\Delta y)^2 \times 10^{-2}$ so that the stability restriction will degrade efficiency. Hence, in the present work an implicit scheme is adopted and non-linear iteration is used for Eqs. (10), (11), and (12)–(13), respectively. This leads to the following discretized problem:

Central differencing Eq. (10) and Eq. (11) at grid point i

and implicitly for time step n , we obtain the pair of tridiagonal systems

$$a_1 U_{i+1}^n + a_2 U_i^n + a_3 U_{i-1}^n = U_i^{n-1} \quad (16)$$

$$b_1 V_{i+1}^n + b_2 V_i^n + b_3 V_{i-1}^n = V_i^{n-1}, \quad (17)$$

where i and n denote space position $x_i = (i-1) \Delta x$, time level $\tau_n = (n-1) \Delta \tau$, and

$$a_1 = \frac{\Delta \tau}{\rho^2} \left[\frac{-1}{2x_i \Delta x} (1 + x_i^2 \rho \dot{\rho}) - \frac{1}{(\Delta x)^2} + \frac{\rho v_1}{2\Delta x} \right] \quad (18)$$

$$a_2 = \frac{\Delta \tau}{\rho^2} \left[\frac{2}{(\Delta x)^2} + \frac{\rho^2}{\Delta \tau} - \rho^2 E^2 \right] \quad (19)$$

$$a_3 = \frac{\Delta \tau}{\rho^2} \left[\frac{1}{2\Delta x x_i} (1 + x_i^2 \rho \dot{\rho}) - \frac{1}{(\Delta x)^2} - \frac{\rho v_1}{2\Delta x} \right] \quad (20)$$

$$b_1 = \frac{-\Delta \tau}{2\rho_1^2 \Delta y} \left[\frac{2}{\Delta y} - \frac{1}{\rho_1^{-1} - y_i} - \rho_1 y_i \dot{\rho} + \frac{v_{II} \Delta \tau}{2\rho_1 \Delta y} \right] \quad (21)$$

$$b_2 = \frac{2\Delta \tau}{\rho_1^2 (\Delta y)^2} + 1 \quad (22)$$

$$b_3 = \frac{-\Delta \tau}{2\Delta y \rho_1^2} \left[\frac{2}{\Delta y} + \frac{1}{\rho_1^{-1} - y_i} + \rho_1 \dot{\rho} y_i - \frac{v_{II} \Delta \tau}{2\rho_1 \Delta y} \right]. \quad (23)$$

Values $\{a_k\}$ and $\{b_k\}$ for the timestep are set initially at the values corresponding to the time level $(n-1)$, and updated iteratively as (16) and (17) are solved by decoupled iteration. Furthermore, v_1 and v_{II} are defined by (12), (13) and in the decoupled iteration we integrate to write

$$v_1 = (U + C_1) \int_0^x \frac{\rho U_\tau}{(U + C_1)^2} dx - \dot{\rho} (U + C_1) \int_0^x \frac{x U_x dx}{(U + C_1)^2} \quad (24)$$

$$v_{II} = (V + C_{II}) \int_0^y \frac{-\rho_1 V_\tau}{(V + C_{II})^2} dy - \dot{\rho} (V + C_{II}) \int_0^y \frac{V_y y}{(V + C_{II})^2} dy, \quad (25)$$

where the expressions on the right are determined from the present iterate. During each iterate, the plasma boundary position ρ is corrected using the condition in Eq. (14). In the

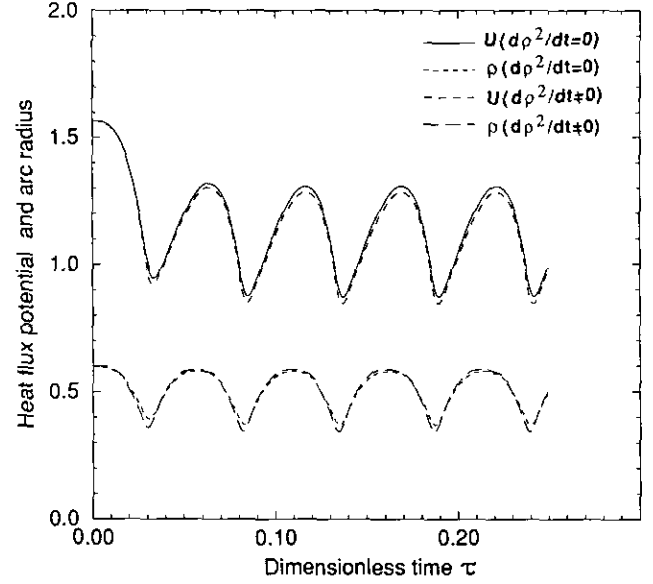


FIG. 2. $d\rho^2/dt$ makes no significant difference for dimensionless heat flux potential U (upper curves) and arc radius ρ (lower curves) when $\omega\theta = 60$ and $\rho_d = 0.6$.

linearized iteration process, values in a_i and b_i are iteratively updated using successive approximation. Iteration proceeds until a specified tolerance ($<10^{-5}$ in the subsequent calculations) on successive iterates is met in each timestep. This decoupling leads to an efficient scheme for the problems of interest here. The calculations below are made using a fixed timestep integration scheme. An adaptive timestep procedure is being developed for computations where $\omega\theta$ is small [6].

Since the boundary position is thermally determined, it is reasonable to expect that sometimes the moving boundary effect is unimportant. Specifically, when ω or θ is large, one expects that there is only a small change in the arc structure. It has been verified theoretically that the perturbation to the arc boundary position decreases as $(\omega\theta)^{-1.5}$ [8]. For example, the comparison of results for heat flux potential U and for arc radius ρ at $\omega\theta = 60$ in Fig. 2 indicate that the assumption $d\rho^2/dt = 0$ is reasonable and is therefore assumed in subsequent computations.

5. NUMERICAL RESULTS AND DISCUSSION

In order to compare the convective and non-convective cases, we define the departure value δA for a quantity A by

$$\delta A = \frac{2 |\langle A_n \rangle - \langle A_c \rangle|}{|\langle A_n \rangle + \langle A_c \rangle|},$$

where $\langle \cdot \rangle$ denotes the time averaged value and subscripts

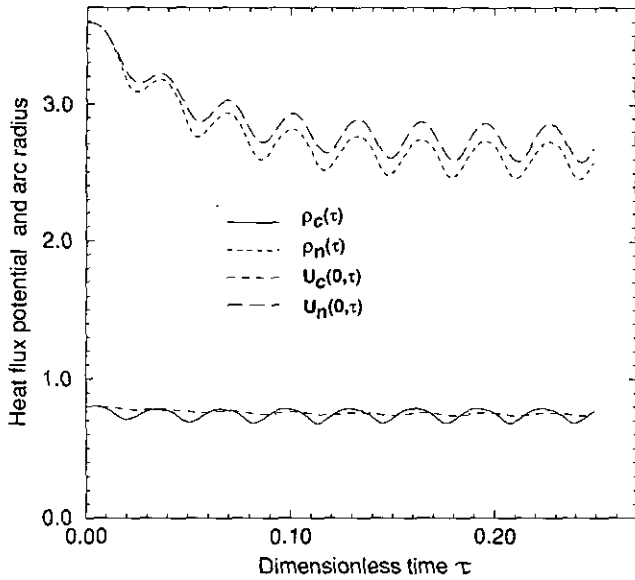


FIG. 3. Heat flux U_c (convective), U_n (nonconvective) and arc radius ρ_c , ρ_n for $\omega\theta = 100$, $\rho_d = 0.8$.

n and c denote non-convection and convection cases, respectively.

As a first test problem let us consider the cases of an arc with $\rho_c = 0.8$ and $\rho_c = 0.6$, respectively; at $\rho_c = 0.8$ with $\omega\theta = 100$, 60, and 20, the energy distributions at the arc center and boundary positions of the arc change in quite different ways (see Figs. 3–5). In particular, we see that the fluctuation δU increases from 5% to 20% and $\delta\rho$ from 10% to 30% when the dimensionless frequency is reduced from 100 to 20. Meanwhile, the (convection) arc boundary

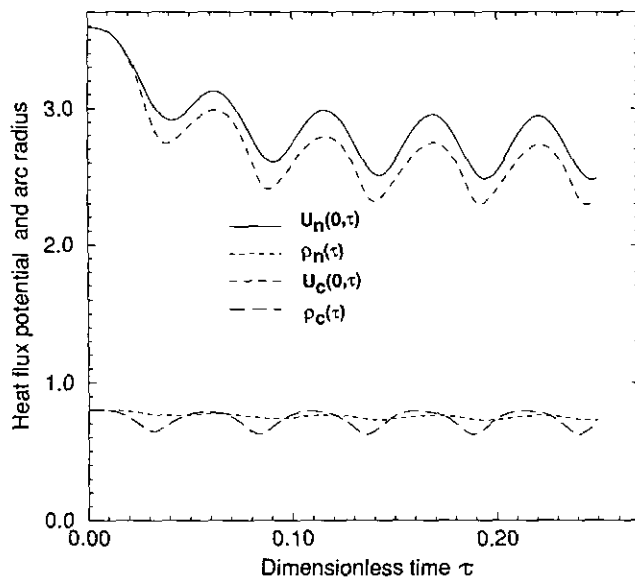


FIG. 4. Heat flux U_c (convective), U_n (nonconvective) and arc radius ρ_c , ρ_n for $\omega\theta = 60$, $\rho_d = 0.8$.

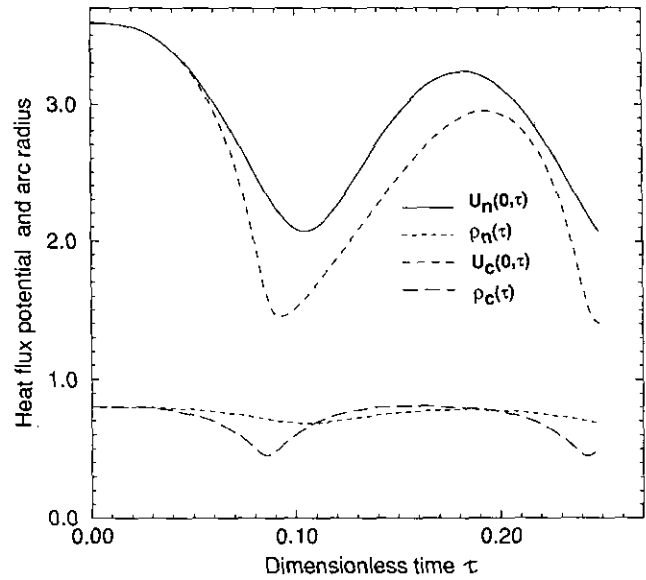


FIG. 5. Heat flux U_c (convective), U_n (nonconvective) and arc radius ρ_c , ρ_n for $\omega\theta = 20$, $\rho_d = 0.8$.

oscillates with greater amplitude than that of the (non-convection) arc. Hence it follows that convection may play an important role in regard to arc boundary movement, especially for low frequency arcs.

At $\rho_c = 0.6$, with $\omega\theta = 100$, 60, 20, the results in Figs. 6–8 lead to the following interesting observation: when the dimensionless frequency $\omega\theta = 20$, arc disruption may occur for $\rho_d = 0.6$ (see Fig. 8, where ρ_c is a minimum) due to the influence of convection, but the arc can work stably when $\rho_d = 0.8$ (recall Fig. 5). A possible interpretation is that a

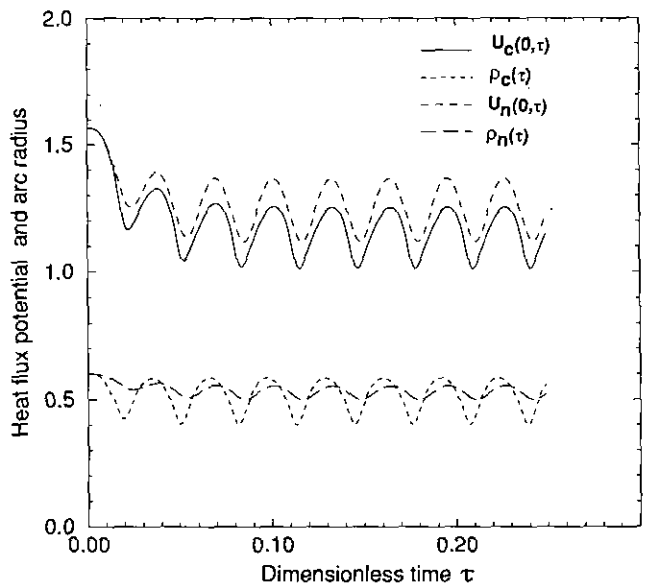


FIG. 6. Heat flux U_c (convective), U_n (nonconvective) and arc radius ρ_c , ρ_n for $\omega\theta = 100$, $\rho_d = 0.6$.

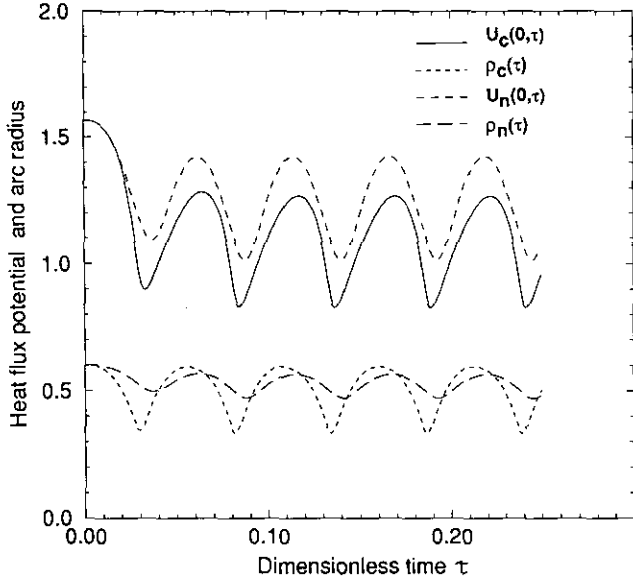


FIG. 7. Heat flux U_c (convective), U_n (nonconvective) and arc radius ρ_c, ρ_n for $\omega\theta = 60, \rho_d = 0.6$.

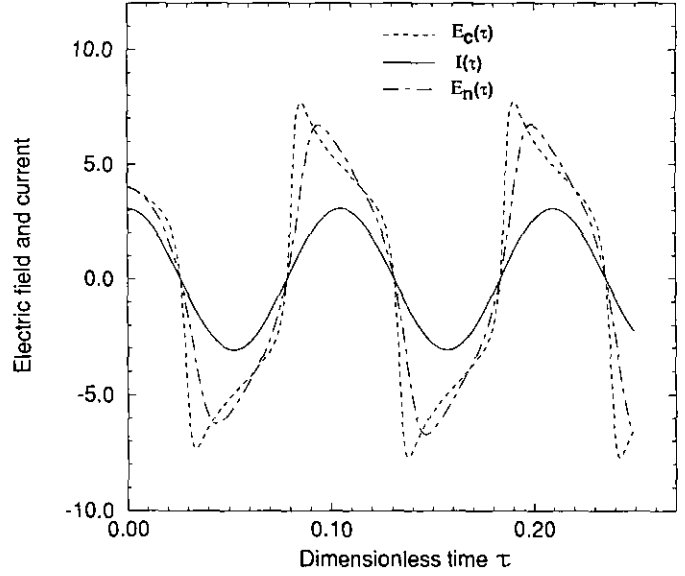


FIG. 9. Electric field E_c (convective), E_n (nonconvective) and current I for $\omega\theta = 60, \rho_d = 0.6$.

thicker arc has a greater thermocapacity which prevents the arc temperature from dropping too rapidly during the current-zero regime. This would enhance arc stability.

The results in Figs. 3–8 indicate that U_c is slightly smaller than U_n in all cases since energy is also transported through convection in the former case and the internal energy is lower. The results also suggest that there is a slight phase shift between the respective solutions for the convective and non-convective cases (as one might anticipate in view of

thermo-inertia). The arc boundary phase shift appears to be more significant and the underlying mechanism warrants further study.

Some interesting results concerning the variation in electric field strength can be deduced from Figs. 9–12. When convection is included, the electric field displays a more sharply rising behavior immediately following the current zero passages than in the model excluding convection. The convective result for the electric field is “flatter” and is in

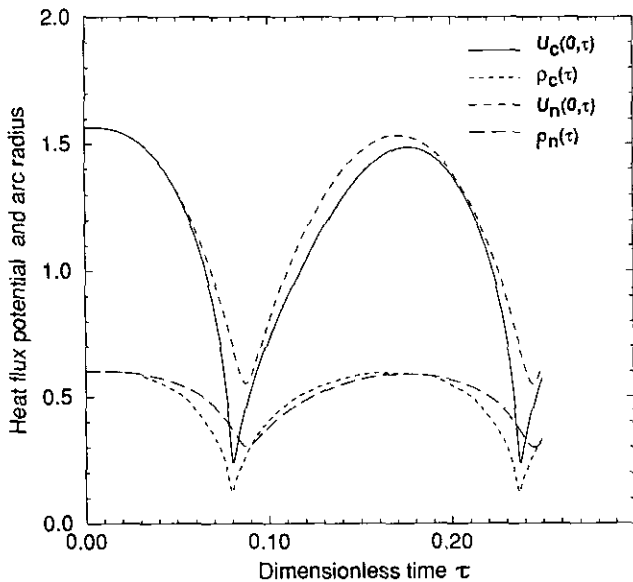


FIG. 8. Heat flux U_c (convective), U_n (nonconvective) and arc radius ρ_c, ρ_n for $\omega\theta = 20, \rho_d = 0.6$.

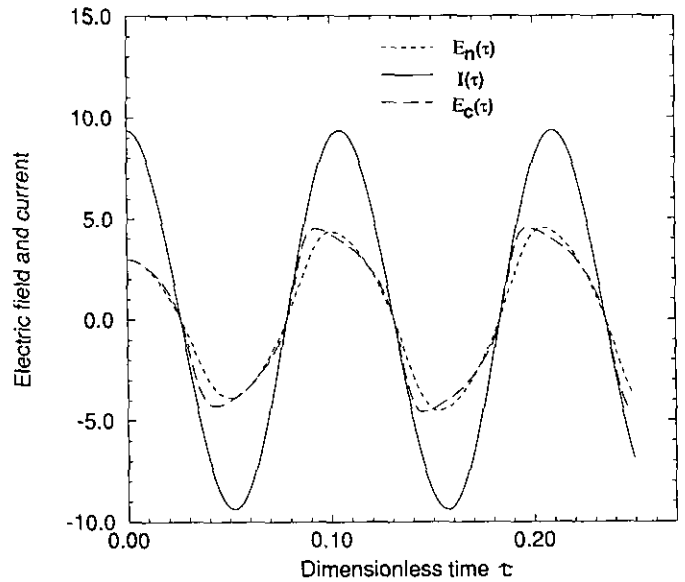


FIG. 10. Electric field E_c (convective), E_n (nonconvective) and current I for $\omega\theta = 60, \rho_d = 0.8$.

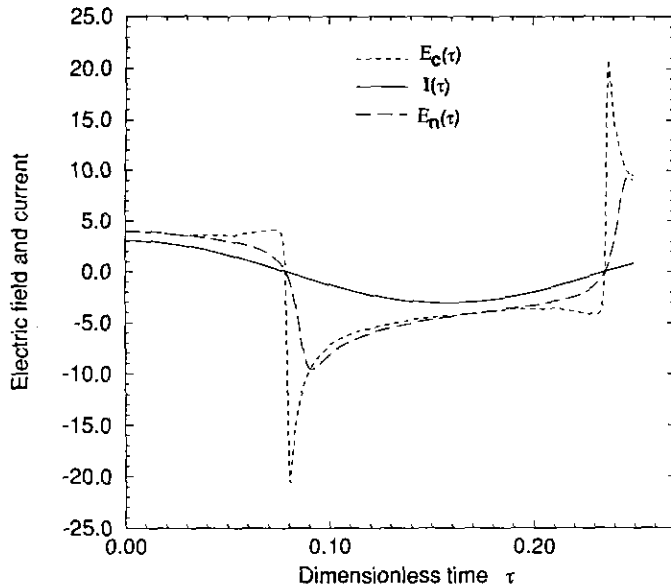


FIG. 11. Electric field E_c (convective), E_n (nonconvective) and current I for $\omega\theta = 20$, $\rho_d = 0.6$.

better agreement with the experimental result [11]. We can interpret this as follows: the underlying physics implies that, since the current is specified, the electric field required to produce this electron flux in a smaller cross section should become larger and remain so until enough energy has been added to appreciably increase the column conductance. In

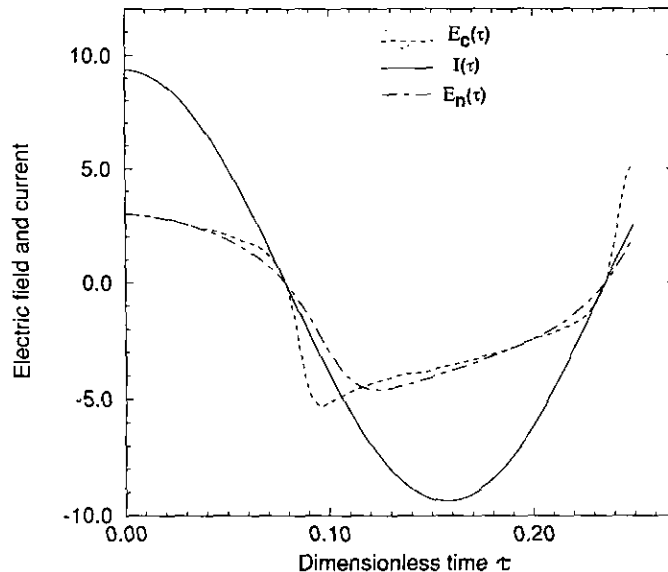


FIG. 12. Electric field E_c (convective), E_n (nonconvective) and current I for $\omega\theta = 20$, $\rho_d = 0.8$.

fact, it is because the radius becomes smaller that a higher electric field is needed to support the specified electric current. In other words, convection makes the boundary of the arc oscillate to smaller radius values so the specified current has to be maintained by a stronger electric field.

6. CONCLUDING REMARKS

In order to study the properties of a dynamic arc at higher current levels, some limitations of the present analysis must be removed. In particular, the radiative term should be included in the energy equation. Also, at some current level the strength of the self-induced magnetic field will become significant and a coupling between the energy equation and the continuity equation with Maxwell's equation will result. The introduction of the integral average $\bar{\kappa}$ in $S = \bar{\kappa}T$ will also restrict the utility of the model (although it facilitates comparison with previous work involving nonconvective models). Finally, the solution in the present study is not appropriate for thermally fast or low-frequency arcs. Studies are now in progress using a time-adaptive scheme to examine these effects [6].

ACKNOWLEDGMENTS

The authors are grateful to Jing-long Wu and Jia-qi Dong for their helpful comments. We gratefully acknowledge the support of the K. C. Wang Education Foundation (Hong Kong) and the Department of Energy.

REFERENCES

1. R. L. Phillips, *Brit. J. Appl. Phys.* **18**, 65 (1967).
2. W. G. Brown, "Basic Theory and Economics of Three-Phase AC Arc Plasma Reactor," in *Proceedings International Conference on Plasma Science and Technology, Beijing, June 1986*, p. 266.
3. K. Ragaller, W. Egli, and K. P. Brand, *IEEE Trans. Plasma Sci.* **PS-10** (3), 154 (1982).
4. R. R. Mitchell, D. T. Tuma, and J. F. Osterle, *IEEE Trans. Plasma Sci.* **PS-13** (14), 207 (1985).
5. M. T. C. Fang and W. H. Bu, *IEEE Proc. A* **138**, 71 (1991).
6. H.-M. Wu and G. F. Carey, *IEEE Trans. Plasma Sci.* **20**, 1041 (1992).
7. H.-M. Wu and Y. M. Chen, "The Non-linear Convective Effect for AC Arc with Moving Boundary," in *Proceedings, 4th Conf. Plasma Tech. of China, Shanghai, 32, 1987*.
8. R. Mclay and G. F. Carey, *Int. J. Numer. Methods Fluids* **9**, 713 (1989).
9. R. Sheng, "On Properties of an AC Arc with Moving Boundary," in *Proc. Int. Conf. on Plasma Sci. and Technol. June 4-7, Beijing, 1986*, p. 101.
10. C. H. Flurscheim, *Power Circuit Breaker Theory and Design* (Peter Peregrinus, 1984).
11. J. D. Cobine, *Gaseous Conductors* (Dover, New York, 1958).